31st Congress of the International Council of the Aeronautical Sciences
Belo Horizonte, Brazil; September 09-14, 2018

WIND SHEAR PARAMETER ESTIMATION FOR DYNAMIC SOARING WITH UNMANNED AERIAL VEHICLES

Duoneng Liu*,Xianzhong Gao**
*** China Aerodynamics Research and Development Center**
****National University of Defense Technology, China**

Keywords: *wind field estimation, unmanned aerial vehicles, dynamic soaring*

Abstract

Unmanned Aerial Vehicles (UAVs) can significantly make use of wind shear to extract energy by the flight technique named dynamic soaring. Wind shear in the field is the necessary condition for dynamic soaring and has a significant impact on the performance of dynamic soaring. Thus, it is important for the on-board auto-pilot of UAV to obtain the estimates of wind shear in real-time. In order to achieve this aim, a method to estimate the wind field is proposed from a new perspective in this paper: the parameters of wind field can be treated as unknown parameters in the flight model of UAVs, and then, the problem to estimate the wind field can be transformed to estimate the unknown parameters in the flight model. For the problem to estimate the unknown parameters in the nonlinear flight model exhibiting Gaussian behavior, a particle filter is developed, and evaluated through its application on dynamic soaring. The results show that the proposed particle filter framework can estimate the unknown parameters in wind field more accurately, reliably and robustly than that of extended Kalman filter.

1 Introduction

In recent years, Unmanned Aerial Vehicles (UAVs) represent one of the most interesting technologies in aeronautics [1]. Meanwhile, the major handicap associated with UAVs is the limited on-board energy capacity [2, 3], and the energy supplement has already been the crucial constraint for the development of UAVs [4, 5]. However, albatrosses can fly long distances even around the world almost without flapping their wings, which means that they are flying nearly at no mechanical cost [6]. After long time observations, people gradually find that albatrosses are particularly adept at exploiting a special maneuver when they are flying in wind shear. This maneuver is named as dynamic soaring, which is defined as a flying technique used to gain kinetic energy without effort by repeatedly crossing the wind shear [7].

Like albatrosses, UAVs may be programmed to perform dynamic soaring autonomously to extract energy from wind shear. If the knowledge of wind field is assumed to be already known, then the energy extraction process can be cast as a trajectory optimization problem [8], such as the works of Deittert et al. [9, 10] and Sachs et al. [11, 12]. However, this assumption will not be available during flight. Moreover, there are currently no sensors that can be carried on a small UAVs to measure the 3D wind field ahead of the UAVs [13], thus it is important for the on-board auto-pilot of UAVs to be able to map or estimate the wind field in real-time using only on-board measurements.

In order to achieve this goal, many scholars have paid great efforts to the on-line estimation method of the wind field. Lawrance et al. [14-16] have described a method for wind field estimation based on Gaussian Process Regression. Langelaan et al. [8, 13] seek to develop a method for wind field estimation that uses known structure to simplify estimation, and

the parameter estimation can be implemented by linear Kalman filter.

Based on their pioneering works, in this paper, an estimator based on the flight model of UAVs is proposed to estimate the wind field in dynamic soaring. The parameter of wind field is treated as the unknown parameter in the model. The particle filter (PF) framework that estimates the unknown parameter of wind field with both constant and time-varying parameter is evaluated through its application in dynamic soaring, and the results of the extended Kalman filter (EKF) are presented for comparison.

2 Models for Wind Estimation

2.1 Wind Shear Model

In order to describe the wind shear above the water surface and at ridges, the exponential model, which has been adopted by Sachs et al. [12, 17], is simply formulated as

$$V_{\mathrm{W}}(h) = V_R\left(h / H_R\right)^p \tag{1}$$

where h is the altitude, V_{w} is the speed of wind which is the function of altitude, H_R is the reference height, V_R is the wind speed at reference height, p is the unknown parameter, which denotes the reference value that is used to indicate the strength of wind shear and to take the properties of the surface into account.

2.2 Flight Model of UAVs

The same as Deittert's model [10], a 6 degree of freedom (DOF) model of UAVs is adopted in this paper, and it is supposed that a linear wind shear is always blowing along x-axis. The definitions of the forces and angles used in this model are shown in Fig.1 where V_{XY} represents the projection of velocity of aircraft on XY-plane, Ψ is the azimuth measured clockwise from Y-axis and γ is flight path pitch angle.

The 6 DOF equations of motion for UAVs are given as follows, where the speed of an aircraft is modeled in a wind relative reference frame and the position of aircraft is modeled in an earth fixed frame, which is defined as the inertial reference frame. V is airspeed, x and y

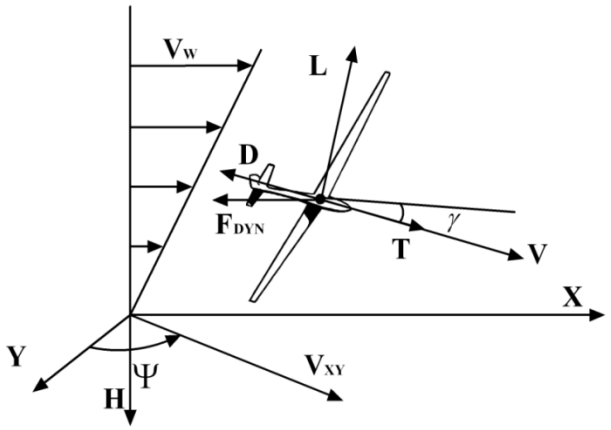

Fig. 1. Forces Acting on UAVs.

are positions, μ is bank angle, L is lift force, D is drag force, T is the thrust.

$$m\dot{V} = T - D - mg\sin\gamma - m\dot{V}_W\cos\gamma\sin\Psi \tag{2}$$

$$mV\cos\gamma\dot{\Psi} = L\sin\mu - m\dot{V}_W\cos\Psi \tag{3}$$

$$mV\dot{\gamma} = L\cos\mu - mg\cos\gamma + m\dot{V}_W\sin\gamma\sin\Psi \tag{4}$$

$$\dot{h} = V\sin\gamma \tag{5}$$

$$\dot{x} = V\cos\gamma\sin\Psi + V_W(h) \tag{6}$$

$$\dot{y} = V\cos\gamma\cos\Psi \tag{7}$$

The lift and drag force are expressed as follows

$$L = \frac{1}{2}\rho S_W C_L V^2 \tag{8}$$

$$D = \frac{1}{2}\rho S_W C_D V^2 \tag{9}$$

The drag coefficient C_D depends on the lift coefficient C_L, yielding

$$C_D = C_{D0} + KC_L^2 \tag{10}$$

where C_{D0} is the zero-lift drag coefficient, K is the induced drag factor. As described in [10], a fictitious force F_{DYN} appears in equations (2)-(7) since the wind relative frame is not inertial:

$$\begin{aligned} F_{DYN} &= -m\dot{V}_W \\ &= -m\left(pV_R / H_R\right)\left(h / H_R\right)^{p-1} V\sin\gamma \end{aligned} \tag{11}$$

It can be seen clearly from equation (11) that the magnitude of F_{DYN} is completely decided by the parameters and states of UAVs, as well as the parameters of wind field. From this viewpoint, the parameters of wind field can be treated as the unknown parameters in the

flight model of UAVs, consequently, the problem to estimate the wind field can be transformed to estimate the unknown parameters in the flight model of UAVs.

3 Augmented Particle Filter

3.1 Augmented System Formulation

It can be known from equations (2)-(7) that the dynamic equation of aircraft is affected by the wind shear. As such, it is possible to estimate the parameter of wind shear through the sensor measurements of aircraft, such as airspeed meter, inertial navigation system (INS), Global Position System (GPS) and so on. In this work, the nonlinear dynamic equations (2)-(7) can be described by the ordinary differential equation

$$\dot{\mathbf{x}}(t)=\mathbf{f}\left[\mathbf{x}(t),\mathbf{u}(t),t\right]+\mathbf{w}(t) \qquad (12)$$

where the vector **f** is a nonlinear function of the state **x**, control input **u** and time t.

The discrete form of equation (12) can be expressed as

$$\mathbf{x}_k=\mathbf{x}_{k-1}+\Delta T\left(\mathbf{f}\left[\mathbf{x}_{k-1},\mathbf{u}_{k-1},k-1\right]+\mathbf{w}_{k-1}\right) \qquad (13)$$

where ΔT is the discrete time, and then the state is defined as

$$\mathbf{x}_k=\begin{bmatrix}V_k & \Psi_k & \gamma_k & h_k & x_k & y_k & p_k\end{bmatrix}^T \qquad (14)$$

where the parameter p_k has been augmented as states to the dynamic system, and then the procedure can be reduced to a pure states estimation problem [18].

The control input is defined as

$$\mathbf{u}_k=\begin{bmatrix}C_{Lk} & \mu_k\end{bmatrix}^T \qquad (15)$$

The disturbance input **w** is a white, zero-mean Gaussian random process, i.e.

$$E\left[\mathbf{w}_k\right]=0,\ E\left[\mathbf{w}_k\mathbf{w}_j^T\right]=\mathbf{Q}\delta(k-j) \qquad (16)$$

where E denotes the expected value of the function, and **Q** is the spectral density matrix, δ is the Dirac delta function.

The expected values of the initial state and its covariance are assumed known:

$$E\left(\mathbf{x}_0\right)=\hat{\mathbf{x}}_0,\ E\left[\left(\mathbf{x}_0-\hat{\mathbf{x}}_0\right)\left(\mathbf{x}_0-\hat{\mathbf{x}}_0\right)^T\right]=\mathbf{P}_0 \qquad (17)$$

The relevant measurements of aircraft are the local airspeed V measured by the airspeed meter and the position vector by the GPS in inertial frame, $[x\ y\ h]^T$. Considered here is the discrete measurement of the form, the measurement equation can be expressed as

$$\mathbf{z}_k=\mathbf{h}\left[\mathbf{x}_k\right]+\mathbf{n}_k,\ \mathbf{h}\left[\mathbf{x}_k\right]=\begin{bmatrix}V_k & x_k & y_k & h_k\end{bmatrix}^T \qquad (18)$$

The measurement noise **n** is assumed to be a white, zero mean Gaussian random process that is uncorrected with the disturbance input:

$$E\left(\mathbf{n}_k\right)=0,\ E\left(\mathbf{n}_k\mathbf{n}_k^T\right)=\mathbf{R}_k,\ E\left[\mathbf{w}(t)\mathbf{n}_k^T\right]=0 \qquad (19)$$

where $\mathbf{R}_k$ is the spectral density matrix of measurement noise.

For the given dynamic equation (13) and measurement equation (18), the problem to estimate the wind shear can be formulated as the problem of sequentially estimating the states $\mathbf{x}_k$ and unknown parameter p in equation (1) when the new observation $\mathbf{z}_k$ is obtained.

3.2 Overview of Particle Filtering Algorithm

The PF estimates the state of the aircraft using available observations expressed in equation (18). It approximates a posteriori probability density function (PDF) by a set of particles, $\mathbf{x}_k^i$, and their associated weights, $\boldsymbol{\omega}_k^i \geq 0$ and $\sum_{i=1}^{N}\boldsymbol{\omega}_k^i=1$, in a discrete summation form [19]:

$$\hat{p}\left(\mathbf{x}_k\left|\mathbf{z}_{1:k}\right.\right)=\sum_{i=1}^{N}\boldsymbol{\omega}_k^i\delta\left(\mathbf{x}_k-\mathbf{x}_k^i\right) \qquad (20)$$

where N is the number of particles. The weights $\boldsymbol{\omega}$ are defined to be as follows:

$$\boldsymbol{\omega}_k^i\propto\boldsymbol{\omega}_{k-1}^i\frac{p\left(\mathbf{z}_k\left|\mathbf{x}_k^i\right.\right)p\left(\mathbf{x}_k^i\left|\mathbf{x}_{k-1}^i\right.\right)}{q\left(\mathbf{x}_k^i\left|\mathbf{x}_{k-1}^i,\mathbf{z}_k\right.\right)} \qquad (21)$$

where $q\left(\mathbf{x}_k^i\left|\mathbf{x}_{k-1}^i,\mathbf{z}_k\right.\right)$ is a proposal distribution called as the importance density. The $q\left(\mathbf{x}_k^i\left|\mathbf{x}_{k-1}^i,\mathbf{z}_k\right.\right)$ plays an important role in the performance of PF, and ideally it should be

equivalent with the true posterior distribution $\hat{p}(\mathbf{x}_k|\mathbf{z}_{1:k})$. However, it is not known in general, and this will be further discussed below.

With these particles $\mathbf{x}_k^i$ and associated weights, the estimated state vector $\hat{\mathbf{x}}_k$ can be calculated as follows

$$\hat{\mathbf{x}}_k = \sum_{i=1}^{N} \mathbf{x}_k^i \hat{p}(\mathbf{x}_k|\mathbf{z}_{1:k}) = \sum_{i=1}^{N} \boldsymbol{\omega}_k^i \mathbf{x}_k^i \quad (22)$$

As discussed above, the optimal importance density function that minimizes the variance of importance weights is

$$q(\mathbf{x}_k^i|\mathbf{x}_{k-1}^i, \mathbf{z}_k) = \hat{p}(\mathbf{x}_k|\mathbf{z}_{1:k}) \quad (23)$$

This optimal importance density is not known in general, one popular suboptimal choice is the transitional prior [18]:

$$q(\mathbf{x}_k|\mathbf{x}_{k-1}^i, \mathbf{z}_k) = p(\mathbf{x}_k|\mathbf{x}_{k-1}^i) \quad (24)$$

If it is furthermore assumed that the process noise is additive zero-mean Gaussian noise, then the PF can propagate the state estimate using the system model:

$$\mathbf{x}_k^i \sim \mathrm{N}(f(\mathbf{x}_{k-1}^i, \mathbf{u}_{k-1}), \mathbf{Q}_{k-1}) \quad (25)$$

Taking equation (24) into equation (21), the new measurements can be combined with the propagated estimate of state in equation (25) to generate the updated estimate of state via the weights:

$$\boldsymbol{\omega}_k^i \propto \boldsymbol{\omega}_{k-1}^i p(\mathbf{z}_k|\mathbf{x}_k^i) \quad (26)$$

$$\hat{\mathbf{x}}_k \approx \sum_{i=1}^{N} \boldsymbol{\omega}_k^i \mathbf{x}_k^i \quad (27)$$

In fact, the role of the weights $\boldsymbol{\omega}$ in PF is similar to the gain in Kalman Filter. The weight is defined in the way that it minimizes the estimation error covariance after the update, and it can be used to combine the propagated estimate with the new measurement. After above discussing, the process of PF to estimate the state in equation (12) can be summarized as

- **Step1**. Initialization：

At time $k = 0$, generating initial particles $\{\mathbf{x}_0^i\}_{i=1}^N$ from the priori distribution $p(\mathbf{x}_0)$, and set $\boldsymbol{\omega}_0^i = 1/N$, $k = 1$.

- **Step2**. Importance sampling:

The value of each particle is estimated by the propagation of system model alone, i.e., it is estimated before the observation is considered

$$\{\mathbf{x}_k^i\}_{i=1}^N \sim \mathrm{N}(f(\mathbf{x}_{k-1}^i, \mathbf{u}_{k-1}), \mathbf{Q}_{k-1}) \quad (28)$$

- **Step3.** Weighting:

The weight of each particle is evaluated by equation (26) when the new measurement is available, and normalize the weight as

$$\bar{\boldsymbol{\omega}}_k^i = \boldsymbol{\omega}_k^i / \sum_{j=1}^{N} \boldsymbol{\omega}_k^j \quad (29)$$

- **Step4**. Re-sampling:

The estimation of each particle is corrected based on weighting information in equation (29) and re-sampling strategy. Then, set $\boldsymbol{\omega}_0^i = 1/N$.

- **Step5**. Output:

The estimation of state is calculated by equation (22), set $k = k+1$ and go back to **Step 2**.

4 Wind Shear Parameter Estimation

4.1 Dynamic Soaring Simulation

The trajectory patterns of dynamic soaring are decided by the different terminal constraints. Zhao [20] has classified the trajectories of dynamic soaring into two patterns: loiter pattern and traveling pattern. Taking the loiter pattern and its constrains as the example, the trajectories of dynamic soaring can be calculated according to the direct collocation approach with the software program AMPL and IPOPT [21, 22] and the the flight model's parameters in equation (2)-(7) are given in Table 1. The trajectory is then tracked by a UAV model using the LQR-based controller in the flight simulation performed in Matlab/Simulink. By Introducing the process noise and measurement noise into dynamic soaring flight, Monte Carlo simulation is performed to get simulative sensor measurements. Then the sensor measurements are used for wind field estimation.

Table 1. The Flight Model's Parameters

Parameter	Value	Unit	Explanation
m	81.7	kg	Mass
S_w	4.2	m^2	Wing area
K	0.045	-	Lift induced drag factor
C_{D0}	0.00873	-	Parasitic drag coefficient
n_{max}	5	-	Max load factor
μ_{max}	75	°	Max bank angle
γ_{max}	70	°	Max flight-path angle
C_{Lmax}	1.5	-	Max lift coefficient
H_R	10	m	Reference altitude
V_R	0.637	m /s	Wind speed at H_R

4.2 Constant Unknown Parameter Estimation

In the simulated dynamic soaring process of this section, the true value of parameter p is assumed to be a constant and equal to 1. The covariance matrix of measurement noise in equation (18) is set as follows:

$$E\left(\mathbf{n}\mathbf{n}^T\right) = \mathrm{diag}\left(n_V^2 \quad n_h^2 \quad n_x^2 \quad n_y^2\right) = \mathrm{diag}\left(1 \quad 5 \quad 5 \quad 5\right) \tag{30}$$

The simulated measurements are shown in Figs. 2 and 3. The covariance matrix of process noise in equation (16) is set as follows:

$$E\left(\mathbf{w}\mathbf{w}^T\right) = \mathrm{diag}\left(w_V^2 \quad w_\Psi^2 \quad w_\gamma^2 \quad w_h^2 \quad w_x^2 \quad w_y^2 \quad w_p^2\right) = \mathrm{diag}\left(2 \quad 0.17 \quad 0.17 \quad 5 \quad 5 \quad 5 \quad 0.2\right) \tag{31}$$

During the estimation process the initial parameter in equation (1) is assumed unknown:

$$E\left(p_0\right) = 0, \; E\left(p_0 p_0\right) = Q_{p0} \tag{32}$$

The Q_{p0} in equation (32) is the covariance of the initial parameter p_0, and the Q_{p0} equals to 10 in the simulation, which indicates there are less confidence to believe that the $E(p_0)$ in equation (32) is the true initial value of the parameter.

To undertake a fair comparison, both the EKF and PF are implemented in recursive form. The estimation results for parameter p in Fig.4 and the relevant results of wind speed in Fig. 5 indicate that the PF converges to the actual value after about 2s. However, the slow convergence of EKF results in a poor performance in estimating the wind field.

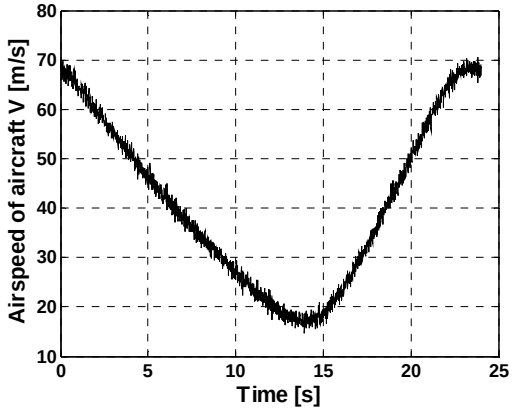

Fig. 2. The Measurement of the Airspeed with Constant Parameter.

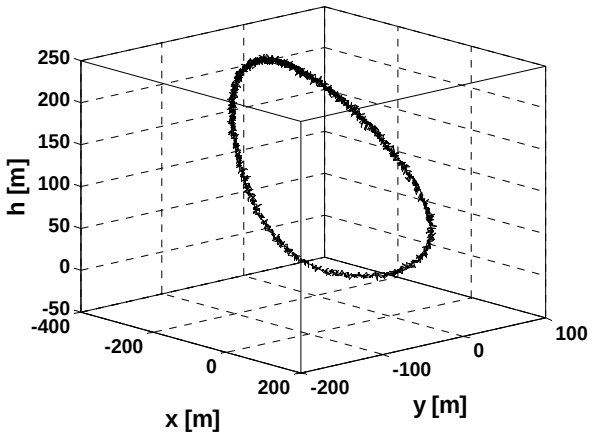

Fig. 3. The Measurement of the Position with Constant Parameter.

In order to quantitatively analyze the performance of PF and EKF, the estimated parameter's mean value and σ bound of root mean square error (RMSE) is defined as:

$$\mathrm{RMSE}(t) = \sqrt{\sum_{j=1}^{n}\left(p_j(t) - \hat{p}_j(t)\right)^2} \tag{33}$$

$$M_{RMSE} = \frac{1}{M}\sum_{i=1}^{M}\mathrm{RMSE}_i(t) \tag{34}$$

$$\sigma_{RMSE} = \sqrt{\frac{1}{M-1}\sum_{i=1}^{M}\left(\mathrm{RMSE}_i(t) - M_{RMSE}\right)} \tag{35}$$

where n is the dimension of parameter p, here $n = 1$; M is the times of realizations, here $M = 40$.

The mean value of RMSE(t) in Fig. 6 shows that, with an incorrect initial value of p_0, the PF can achieve significantly more accurate estimates of p than the EKF. The 1σ bounds for the RMSE(t), based on 40 realizations, also indicate that the PF is more reliable and robust than the EKF.

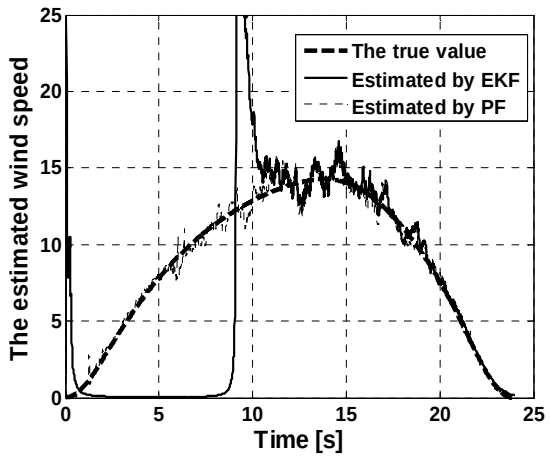

Fig. 4. The Estimated Wind Speed with Constant Parameter.

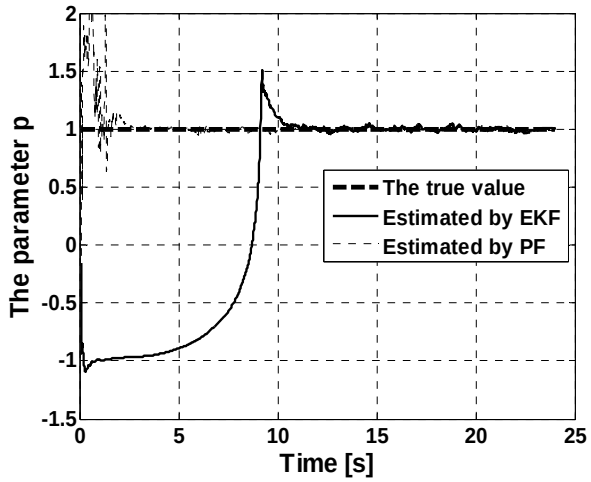

Fig. 5. The Estimated *p* Value with Constant Parameter.

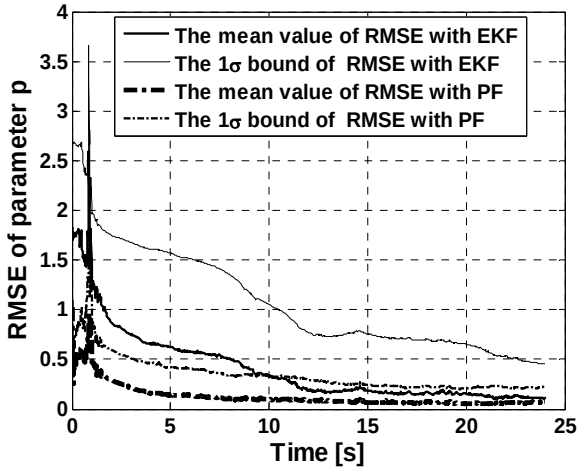

Fig. 6. The Mean Value of RMSE Based on 40 Realizations.

The other issue with the PF applied to the wind field estimation is to decide on the number of particles. The appropriate number of particles is normally determined by the state dimensions, the non-linearity of the system, and the properties of the unknown parameters [23]. In general, the more particles, the better estimation performance can be achieved such that a lower M_{RMSE} with a tighter σ bound. However, the more particles, the more computational load is required. Thus, it is important to keep a balance between the performance and computational load for the application of PF. In order to do so, instead to directly compare the computational load of algorithms by their consumed CPU time, the RMSE, the times of divergence based on 40 realizations, and the ratio of required CPU time by EKF to that by PF with different number of particles are summarized in Table 2, where the RMSE is defined as equation (36), and can be used to indicate the estimation performance of each filter.

$$\mathrm{RMSE} = \frac{1}{T}\int_0^T \mathrm{RMSE}(t)dt \qquad (36)$$

The results in Table 2 are obtained on an Intel®Core™, i3-2100 UP@3.10GHz computer running under Windows XP. They show that the RMSE of PF is inversely-proportional with the number of particles and the CPU time is proportional with the number of particles. When the number of particles is N = 200, the RMSE and CPU time of PF is almost equivalent to that of EKF. The RMSE of PF is greatly reduced compared to EKF when N = 1000, however, the ratio of PF's CPU time to that of EKF will increase to 3.866. As the period of dynamic soaring is about 20 seconds, and the computational ability of on-board computer in UAVs is less than that of the personal computer, how to reduce the computational load of PF and make it suited for the application on the on-board computer still need further research.

Table 2. The Estimation Performance

Filters	EKF	PF			
		N=100	N =200	N =500	N= 1000
RMSE	0.410	1.210	0.359	0.333	0.129
CPU time	1	0.676	1.134	2.279	3.866

4.3 Variable Unknown Parameter Estimation

During dynamic soaring process, the unknown parameter p may vary over time, owing to the specific correlation of the p at a particular location and environment. The factors affecting the variation of parameter p have been studied in [24, 25], the research results show that, the heating and cooling cycle of the air adjacent to the earth during the 24 hours of the day influences the parameter p significantly, on a diurnal basis, wind speeds are higher during the daylight hours and drop to below-average values at night.

Thus, the following study considers an unknown, time-varying parameter p in wind field. To simulate the time-varying effect, the actual value of p is assumed to follow a linear decreasing trend, i.e.:

$$p_k = p_{k-1} + \Delta T\left(-Ak_T\right) \tag{37}$$

where k_T is the time index. The initial value of p is also set as shown in equation (32) whilst the true values in equation (37) are $p_0 = 1$ and $A = 1/48$.

The covariance matrix of measurement noise is the same as that in equation (30).The covariance matrix of process and the initial parameter are the same as those in equation (31).

The estimation results for time-varying parameter in Figs. 7 and 8 clearly indicate that the superior results are attained for the PF. At the beginning of estimation, the oscillations present in the PF are mainly due to the large initial covariance of parameter p_0, which allows the methodology to search over large regions for areas of high probability for the true value of the parameter. Although both the EKF and PF can obtain satisfactory estimates at the end of dynamic soaring, the PF follows the trend of parameter p more quickly and precisely.

5 Conclusions

The method to estimate the wind field is proposed from a new perspective in this paper. The parameters of wind field are treated as the unknown parameters in the flight model of Unmanned Aerial Vehicles (UAVs), and then, the problem to estimate the wind field is transformed to estimate the unknown parameters in the flight model. The application of particle filter (PF) for the on-line wind field estimation in dynamic soaring is then introduced. The unknown parameter is treated as a state and incorporated into the flight model of UAVs to obtain robust estimates. The proposed PF framework is evaluated on the wind field with both constant and time-varying parameters. The results show that the PF framework can estimate the unknown parameters in wind field more accurately, reliably and robustly than that of Extended Kalman Filter. The implications of this study are that particle filters are particularly attractive for applications requiring on-line parameter estimation. Further improvements of the importance density for PF and how to reduce the computational load to be suitable for the application on the on-board computer of UAVs are also under investigation.

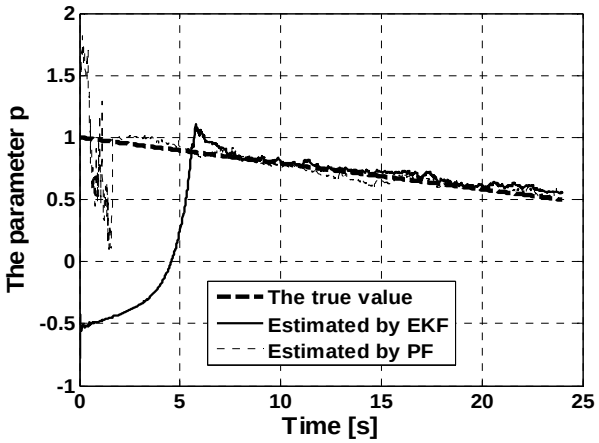

Fig. 7. The Estimated p Value with Variable Parameter.

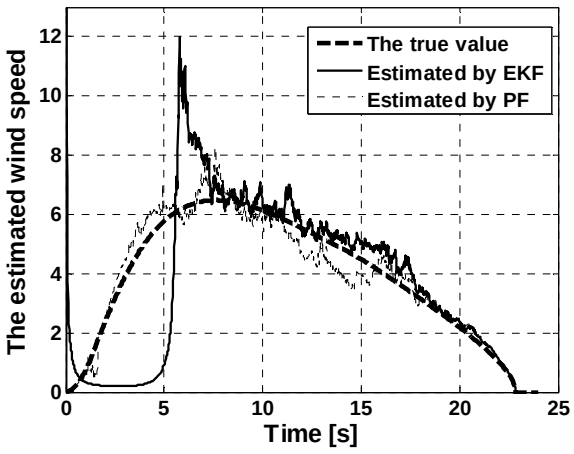

Fig. 8. The Mean Value of RMSE Based on 40 Realizations.

References

[1] Filippis L D, Guglieri G, and Quagliotti F. A minimum risk approach for path planning of UAVs, *Journal of Intelligent and Robotic Systems,* Vol. 61, pp 203-219, 2011.

[2] Langelaan J W. Biologically inspired flight techniques for small and micro unmanned aerial vehicles. *AIAA Guidance, Navigation and Controls Conference*, Honolulu, Hawaii, AIAA Paper 2008-6511, 2008.

[3] Langelaan J W and Bramesfeld G. Gust energy extraction for mini- and micro- uninhabited aerial vehicles. *46th AIAA Aerosciences Conference*, Reno Nevada, AIAA Paper 2008-0223, 2008.

[4] Chakrabarty A. Flight path planning of UAV based on atmospheric energy harvesting. *Master Thesis*, The Pennsylvania State University, USA, 2010.

[5] Depenbusch N T. Atmospheric energy harvesting for small uninhabited by gust soaring. *Master Thesis*, The Pennsylvania State University, USA, 2011.

[6] Sachs G, Traugott J, Nesterova A P*, et al.* Flying at no mechanical energy cost: disclosing the secret of wandering albatrosses. *PLoS ONE,* vol. 7, p e41449, 2012.

[7] Richardson P L. How do albatrosses fly around the world without flapping their wings. *Progress in Oceanography,* vol. 88, pp 46-58, 2011.

[8] Langelaan J W, Alley N and Neidhoefer J. "ind field estimation for small unmanned aerial vehicles. *AIAA Guidance, Navigation and Control Conference*, Toronto, Canada, AIAA Paper 2010-8177, 2010.

[9] Deittert M. Dynamic soaring flight in turbulence. *AIAA Guidance Navigation and Control Conference*, Chicago Illinois, AIAA Paper 2009-6012, 2009.

[10] Deittert M, Richards A, Toomer C A, and Pipe A. Engineless unmanned aerial vehicle propulsion by dynamic soaring. *Journal of Guidance, Control, and Dynamics*, vol. 32, pp 1446-1457, 2009.

[11] Sachs G and Casta O. Dynamic soaring in altitude region below jet streams. *AIAA Guidance, Navigation, and Control Conference and Exhibit*, Keystone Colorado, AIAA Paper 2006-6602, 2006.

[12] Sachs G and Casta O. Optimization of dynamic soaring at ridges. *AIAA Atmospheric Flight Mechanics Conference and Exhibit,* Austin Texas, AIAA Paper 2003-5303, 2003.

[13] Langelaan J W, Spletzer J, Montella C and Grenestedt J. Wind field estimation for autonomous dynamic soaring. *IEEE International Conference on Robotics and Automation*, RiverCentre, Saint Paul, Minnesota , pp 16-22, 2012.

[14] Lawrance N R J and Sukkarieh S. Autonomous exploration of a wind field with a gliding aircraft. *Jouranl of Guidance, Control, and Dynamics*, vol. 34, pp. 719-723, 2011.

[15] Lawrance N R J and Sukkarieh S. Path planning for autonomous soaring flight in dynamic wind fields. *2011 IEEE International Conference on Robotics and Automation*, Shanghai, China, pp 2499-2505, 2011.

[16] Lawrance N R J. Autonomous soaring flight for unmanned aerial vehicles. *PhD Thesis*, The University of Sydney, Australia, 2011.

[17] Sachs G. Minimum shear wind strength required for dynamic soaring of albatrosses. *Ibis*, vol. 147, pp 1-10, 2005.

[18] Olivier L E, Huang B and Craig I K. Dual particle filters for state and parameter estimation with application to a run-of-mine ore mill. *Journal of Process Control*, vol. 22, pp 710-717, 2012.

[19] Shao X, Huang B and Lee J M. Constrained bayesian state estimation – a comparative study and a new particle filter based approach. *Journal of Process Control*, vol. 20, pp 143-157, 2010.

[20] Zhao Y J. Optimal patterns of glider dynamic soaring. *Optimal Control Appication and Methods*, vol. 25, pp 67-89, 2004.

[21] Fourer R, Gay D M and Kernighan B W. *AMPL: a Modeling Language for Mathematical Programming*. Duxbury, MA: Thomson, 2002.

[22] Wächter A and Biegler L T. On the implementation of a primal-dual interior point filter line search algorithm for large-scale nonlinear programming. M*athematical Programming*, Vol. 106, No. 1, pp 25-57, 2006.

[23] Chen T, Morris J and Martin E. Particle filters for state and parameter estimation in batch processes. *Journal of Process Control*, vol. 15, pp 665-673, 2005.

[24] Farrugia R N. The wind shear exponent in a mediterranean island climate. *Renewable Energy*, vol. 28, pp 647-653, 2003.

[25] Rehman S. Wind shear coefficients and their effect on energy production. *Energy Conversion and Management*, vol. 46, pp 2578-2591, 2005

Contact Author Email Address

Contact author: Xianzhong Gao
Mailto: gaoxianzhong@nudt.edu.cn

Copyright Statement